

# Effect of the number of patches on the growth of networks of patchy colloids on substrates

C. S. Dias,<sup>1,\*</sup> N. A. M. Araújo,<sup>1,†</sup> and M. M. Telo da Gama<sup>1,‡</sup>

<sup>1</sup>*Departamento de Física, Faculdade de Ciências,  
Universidade de Lisboa, P-1749-016 Lisboa, Portugal,  
and Centro de Física Teórica e Computacional, Universidade de Lisboa,  
Avenida Professor Gama Pinto 2, P-1649-003 Lisboa, Portugal*

We investigate numerically the irreversible aggregation of patchy spherical colloids on a flat substrate. We consider  $n$ -patch particles and characterize the dependence of the irreversible aggregation kinetics on  $n$ . For all values of  $n$ , considered in this study, the growing interface of the aggregate is in the Kardar-Parisi-Zhang universality class, although the bulk structure exhibits a rich dependence on  $n$ . In particular, the bulk density varies with  $n$  and the network is more ordered for particles with fewer patches. Preferred orientations of the bonds are also observed for networks of particles with low  $n$ .

## I. INTRODUCTION

Colloids with attractive patches on their surface have been under the spotlight due to their possible role in the development of novel materials with fine tuned mechanical, optical, and thermal properties [1–4]. In recent years, many fabrication techniques have been developed [5–11] which motivated the development of a wide range of theoretical models [4, 12–20]. Theoretical [21–25] and experimental [26, 27] studies have revealed a strong dependence of the equilibrium structures of patchy colloids on the valence and the strength of the interactions. After the quest for the feasibility of the equilibrium model structures the emphasis has shifted to the kinetics [25, 28–31] including the adsorption of films on substrates [32–36].

Recent efforts have been focused on the nonequilibrium properties of patchy colloids, with emphasis on the structure of the adsorbed films [34–36] and the properties of the growing interface [37, 38]. In particular, it was shown that, in the limit of irreversible adsorption, growth on substrates is sustained only for certain arrangements of the patches on the surface of the colloids, delimited by two absorbing phase transitions from thin to thick films [37]. It was also found that while for isotropic sticking colloids and single patch-type colloids the growing interface is in the Kardar-Parisi-Zhang universality class [37, 39–41] for colloids with weak and strong bonds the interface is in the universality class of Kardar-Parisi-Zhang with quenched disorder, for significantly distinct energies of the patch-patch interactions [38].

In this work, we study the influence of the number of patches  $n$  on the interfacial and bulk properties of the networks on flat substrates.

In the following section we give a description of the model. In Sec. III, we present our results and in Sec. IV, we draw some conclusions.

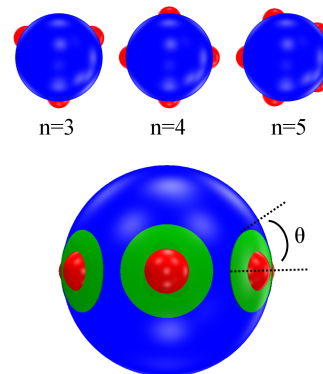


FIG. 1. Bottom: Schematic representation of the patches (red) on the surface of a colloid (blue) and their interaction range (green). The interaction range is defined by an angle  $\theta$  with the center of the patch. This angle controls the extension and strength of the patch. Top: Patchy colloids with three, four, and five patches distributed regularly along the equator of the particle.

## II. MODEL

We consider spherical three-patch colloids of unit diameter  $\sigma$  with short-range attractive patches on their surface. To access large-length and long-time scales, we use a stochastic model first proposed in Ref. [34]. We describe the patch-patch short-range interaction in a stochastic way and we focus on chemical or DNA mediated bonds [10, 42], which are highly directional and very strong. This type of bonds may be considered irreversible within the timescale of interest [43], as we consider here. The high directionality of the interactions is modeled by assuming optimal bonds such that the center of two bonded colloids is aligned with their bonding patches.

As in colloidal aggregation at the edge of drops [44], we consider advective mass transport only. We denote by  $h_{\max}$  the maximum height of a colloid in the aggregate and start the simulation from an empty substrate, i.e.

\* csdias@fc.ul.pt

† nmaraujo@fc.ul.pt

‡ margarid@cii.fc.ul.pt

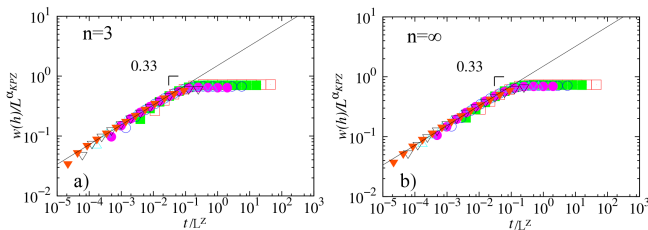


FIG. 2. Data collapse according to the Family-Vicsek scaling relation (2) for (a)  $n = 3$  and (b)  $n = \infty$ . Simulations were performed on substrates of linear sizes ranging from  $L = 32$  to  $L = 2048$  with  $2048L$  adsorbed patchy colloids averaged over  $6.4 \times 10^5$  samples, for the smaller systems, and  $10^4$  samples for the larger ones. We considered  $\alpha_{\text{KPZ}} = 0.5$  and  $z = 1.5$  consistent with the Kardar-Parisi-Zhang universality class [45].

$h_{\text{max}} = 0$ . We choose a horizontal position uniformly at random, at height  $h_{\text{dep}} = h_{\text{max}} + \sigma$ , and simulate the ballistic downward trajectory of the colloid until it hits either the substrate or another colloid. A colloid-substrate collision results on the adsorption of the colloid with a random orientation.

Particle-particle interactions are described, as shown in Fig. 1, by the interaction range (green), on the surface of the colloid (blue), around each patch (red). The range is characterized by a single parameter, namely, its angle  $\theta$  with the center of the patch. In a collision with a pre-adsorbed colloid, bonding occurs when contact is within overlapping interaction ranges. The position of the incoming particle is then adjusted to align the patch-patch orientation with that for optimal bonding. Otherwise, bonding fails, i.e., the colloid is discarded and a new one is released from the top.

### III. RESULTS

In order to investigate the effect of the number of patches  $n$ , we vary  $n$  from  $n = 3$  to  $n = \infty$ . A schematic representation of the particles is depicted in Fig. 1 (top). For  $n = 2$  only independent chains grow and there is no interface. We view this limit ( $n = 2$ ) as the pinned phase. The opposite limit,  $n = \infty$ , corresponds to the aggregation of isotropic sticky colloids [39–41]. We performed detailed simulations for systems with substrate sizes ranging from  $L = 32$  to  $L = 2048$  and averaged over as many as  $6.4 \times 10^5$  samples for the smallest systems and  $10^4$  samples for the largest ones. Below, we analyze the properties of both the interface and the bulk of the adsorbed films. We analyze the scaling of the growing interface (Sec. III A), the pair-distribution function of the colloids in the network (Sec. III B), the density of the bulk (Sec. III C), and the orientation of the bonds (Sec. III D).

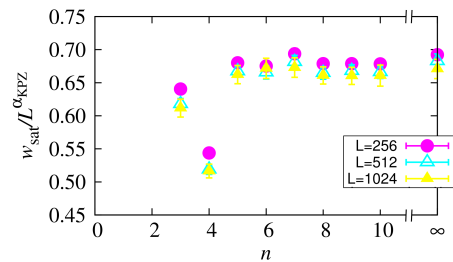


FIG. 3. Data collapse for the saturation roughness dependence on the number of patches  $n = \{3, 4, 5, 6, 7, 8, 9, 10, \dots, \infty\}$ ,  $w_{\text{sat}} = L^{\alpha_{\text{KPZ}}} \mathcal{F}[n]$ , where  $\mathcal{F}$  is a scaling function and  $\alpha_{\text{KPZ}} = 0.5$  is the roughness exponent for the Kardar-Parisi-Zhang universality class. We considered three different substrate lengths  $L = \{256, 512, 1024\}$  and results are averages over  $\{8 \times 10^4, 4 \times 10^4, 2 \times 10^4\}$  samples.

#### A. Interfacial scaling

We start by characterizing the kinetic roughening of the growing interface. We divide the off-lattice system into  $N$  columns of width  $\sigma$ , where  $N = L/\sigma$ . We determine the interfacial height  $h_i$ , of each column  $i$ , and calculate the interfacial roughness  $w$ , defined as,

$$w(t) = \sqrt{\langle [h_i(t) - \langle h(t) \rangle]^2 \rangle}, \quad (1)$$

where  $\langle h(t) \rangle = \sum_i h_i/N$  denotes an average over the  $N$  columns. The time  $t$  is defined as the number of adsorbed layers of colloids (equivalent to the average height used in experiments). Initially, the roughness increases with time but, due the substrate finite size it saturates eventually at a value  $w_{\text{sat}}$  that increases with the system size [45, 46]. The saturation roughness and saturation time ( $t_{\text{sat}}$ ) scale with the system size as  $w_{\text{sat}} \sim L^\alpha$  and  $t_{\text{sat}} \sim L^z$ , respectively, where  $\alpha$  is the roughness exponent and  $z$  is the dynamical exponent. The short-time behavior of the interface roughness is also a power law given by  $w(t) \sim t^\beta$  where  $\beta$  is the growth exponent. The interfacial roughness is expected to follow the *Family-Vicsek* [47] scaling relation,

$$w(L, t) = L^\alpha f\left(\frac{t}{L^z}\right), \quad (2)$$

where  $f(u)$  is a scaling function. Using the scaling relation and the exponents for different universality classes we can identify the universality class of the growing interface.

Figure 2 illustrates the data collapse of the roughness rescaled using the Family-Vicsek scaling relation (2), for two values of the number of patches  $n = \{3, \infty\}$ . The data collapse is obtained using the critical exponents of the *Kardar-Parisi-Zhang* (KPZ) universality class, namely  $\beta = 1/3$ ,  $\alpha = 1/2$ , and  $z = 3/2$ , revealing

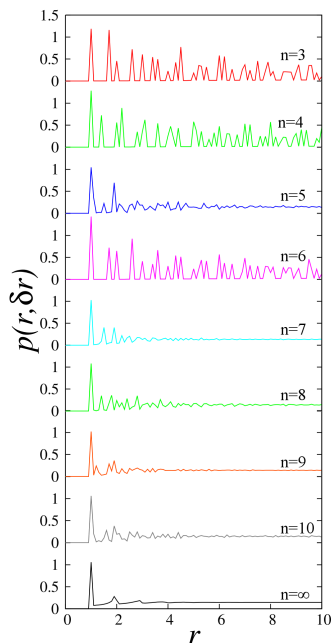


FIG. 4. Pair-distribution function from top to bottom for  $n = \{3, 4, 5, 6, 7, 8, 9, 10, \infty\}$ , given by Equation (3) with  $\delta r = 0.1$ . A system of size  $L = 512$  and  $512L$  deposited colloids was considered with the results averaged over  $10^4$  samples.

that the interface is in this universality class regardless of the anisotropy of the bonding interactions, related to the number of patches. The KPZ scaling is corroborated by the scaling of the saturation roughness for different  $n$ , illustrated in Fig. 3, for three different system sizes. Note that data collapse is obtained when the roughness is rescaled by  $L^{\alpha_{\text{KPZ}}}$ , as expected. This result contrasts to that observed for particles which are asymmetric in shape [44] or bonding energies [38]. We note a remarkable non-monotonic dependence of the roughness on  $n$ , with a rapid variation for low-valence colloids and a minimum at  $n = 4$ , as a result of two distinct mechanisms. While the binding probability, increasing with  $n$  (maximal for isotropic colloids), increases the interfacial roughening there are magic values of  $n$ , which by favouring local order lead to a strong decrease of the interfacial roughness.

### B. Ordered and disordered structures

A quantitative description of the effect of the number of patches on the local structure of the aggregates is obtained from the spatial distribution of the colloids in the network. We used the pair-distribution function  $p(r, \delta r)$  defined as,

$$p(r, \delta r) = \frac{1}{N} \sum_i \sum_{j \neq i} f(|r_{ij} - r|, \delta r) / Nr, \quad (3)$$

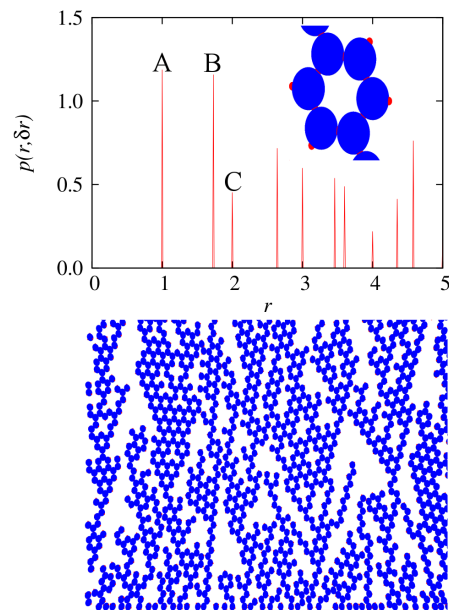


FIG. 5. Top: Pair-distribution function for aggregates of three-patch colloids with  $\delta r = 0.01$ . The peaks A, B, and C are at the distances of the first three neighbors on the honeycomb lattice. A substrate of length  $L = 512$  and  $512L$  aggregated colloids averaged over  $10^4$  samples was used. Top inset: Zoom of a typical local structure in aggregates of three-patch colloids. Bottom: Snapshot of a system with substrate length  $L = 128$  with  $10L$  deposited three-patch colloids.

where  $r$  is the distance between each pair  $ij$  of colloids and  $f(|r_{ij} - r|, \delta r)$  is one if  $|r_{ij} - r| < \delta r$  and zero otherwise. Figure 4 compares the pair-distribution functions of the systems investigated ( $n = 3$  up to  $n = \infty$ ). For colloids with low valence, the interfacial roughness depends strongly on the local structure of the aggregates. As revealed by Fig. 4, the aggregates of colloids with  $n = \{3, 4, 6\}$  exhibit ordered patterns that extend over distances much larger than the particle diameter, while for larger values of  $n$  only local order is observed. For colloids with  $n > 6$ , the aggregates are disordered and the structure approaches that of isotropic colloids,  $n = \infty$ , as  $n$  increases (see bottom of Fig. 4). The latter is characterized by a well defined peak at  $r = 1$  (shell of first neighbors) and weak secondary peaks slightly below  $r = 2$  and  $r = 3$  (shells of second and third neighbors, respectively).

To quantify the order of the colloidal aggregates we re-plot the pair distribution functions in Figs. 5, 6, and 7 with smaller binning, namely,  $\delta r = 0.01$ . Figure 5 shows the pair-distribution function for aggregates of three-patch colloids ( $n = 3$ ). The snapshot at the bottom of Fig. 5 reveals that the local structure of the nonequilibrium aggregate resembles that of a honeycomb lattice. Furthermore, it is clear that the local structure extends over large distances, of the order of the substrate length. The first three peaks of the pair-distribution function, A, B, and C, are at the first, second, and third nearest

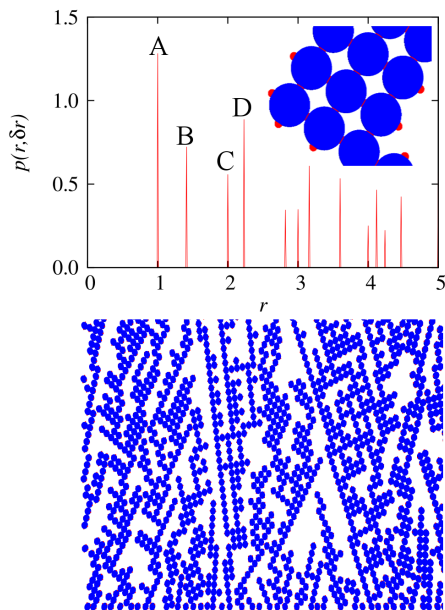


FIG. 6. Top: Pair-distribution function for aggregates of four-patch colloids with  $\delta r = 0.01$ . The peaks A, B, C, and D are at the distances of the first four neighbors on the square lattice. A substrate of length  $L = 512$  and  $512L$  aggregated colloids averaged over  $10^4$  samples was used. Top inset: Zoom of a typical local structure in aggregates of four-patch colloids. Bottom: Snapshot of a system of substrate length  $L = 128$  with  $10L$  deposited four-patch colloids.

neighbor distances on the honeycomb lattice, i.e.,  $r_A = 1$ ,  $r_B = 1.73$ , and  $r_C = 2$ , respectively. The solid-like structure is far from perfect with large irregular voids scattered within ordered domains.

For colloids with  $n = 4$ , local order extending over large distances is also observed (zoom and snapshot in Fig. 6). Since the valence is now four, the local structure is similar to that of the square lattice. The first peaks in the pair-distribution function correspond to the first ( $r_A = 1$ ), second ( $r_B = 1.414$ ), third ( $r_C = 2$ ), and fourth neighbors ( $r_D = 2.236$ ) on the square lattice. The solid-like structure is far from perfect with large irregular voids scattered within ordered domains.

Figure 7 shows the results for colloids with  $n = 6$ . We note that, on the large scale, there is no order. The local order, however, is still well defined (zoom in top inset of Fig. 7). This is confirmed by the pair-distribution function, plotted in Fig. 7, with well defined peaks at distances corresponding to the first three neighbors on the triangular lattice,  $A$  at  $r_A = 1$ ,  $B$  at  $r_B = 1.73$ , and  $C$  at  $r_C = 2$ .

The positions of the first three peaks of the pair-distribution function of six-patch colloids are the same as those of three-patch colloids, as observed in honeycomb and triangular lattices. The relative intensity of the peaks, however, differs in the two types of aggregates, which is also different from the relative intensity of the

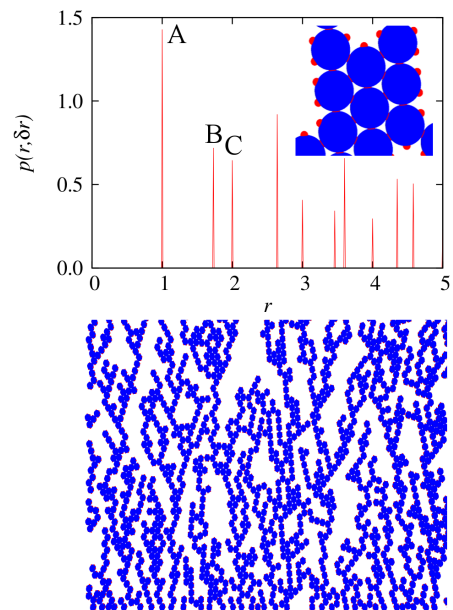


FIG. 7. Top: Pair-distribution function for aggregates of six-patch colloids with  $\delta r = 0.01$ . The peaks A, B, and C are at the distances of the first three neighbors on the triangular lattice. A substrate of length  $L = 512$  and  $512L$  aggregated colloids averaged over  $10^4$  samples was used. Top inset: Zoom of a typical local structure in aggregates of six-patch colloids. Bottom: Snapshot of a system of substrate length  $L = 128$  with  $10L$  deposited six-patch colloids.

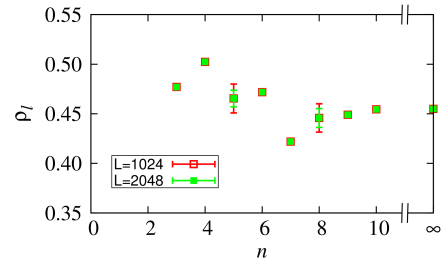


FIG. 8. Density of the film as a function of the number of patches  $n$  for systems of substrate length  $L = \{1024, 2048\}$  and  $2048L$  aggregated colloids averaged over  $10^5$  samples.

peaks in the corresponding lattices. The difference in the intensity of the peaks for systems with valence three and six results from the increase in the number of neighbors with valence, in line with the corresponding lattices.

### C. Network density

One property of practical interest is the network density, which we plot in Fig. 8 as a function of the number of patches  $n$ . We can identify two regimes: one for systems with low valence where ordered structures dominate



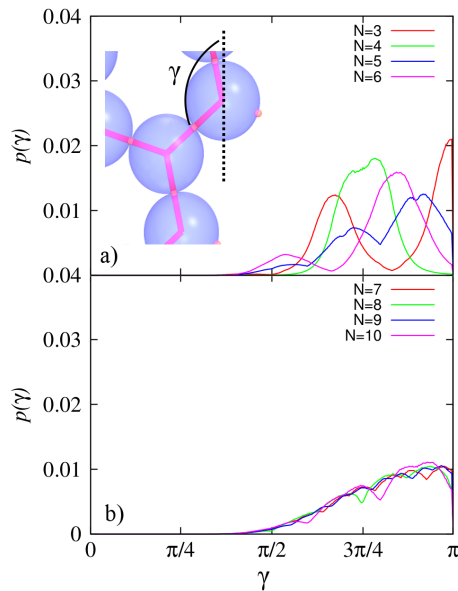


FIG. 9. Probability of the patch-patch bond orientation for a) colloids with  $n = \{3, 4, 5, 6\}$  patches and b) colloids with  $n = \{7, 8, 9, 10\}$  patches. The orientation of the bond is measured with respect to a vertical axis, as shown in the inset of figure a). Simulations were performed for a system of size  $L = 2048$  with  $2048L$  deposited colloids and averaged over  $10^5$  samples.

and the other where the aggregates are amorphous. In the ordered regime, the density changes abruptly with  $n$ . The density has a maximum at  $n = 4$  due to compactness of the local structures when compared with those at  $n = 3$ . It decreases for  $n = 5$  as no ordered structures form. For systems with  $n = 6$  the density increases again as a result of local triangular structures. However, the effects of the growth kinetics destroys the global order and thus the density is significantly lower than for  $n = 3$  and  $n = 4$ . Locally the voids may appear larger, as from the snapshots of both Figs. 5 and 6, however ordered structures are less affected by fluctuations in the structure. On the other hand, for amorphous-like structures the fluctuations in the aggregate structures are higher and large scale voids are more common, which decreases the global density of the network. We note that the density dependence on  $n$  is opposite to that of the roughness. In fact, denser structures reduce the fluctuations of the interfacial height, which in turn decrease the roughness. For amorphous films, however, both the density and the roughness increase slightly as  $n$  increases, below the limit of isotropic colloids  $n = \infty$ .

#### D. Bond orientation

Finally we address the orientation of the bonds between patches. This analysis gives insight into the kinetics of growth of the network of patchy colloids. We

consider a vertical  $y$  axis on the two dimensional system, as shown in the inset of Fig. 9(a) (dashed line) and compute the distribution function of the angle between the bond and this direction. The results plotted in Fig. 9, reveal that for systems with low valence,  $n < 7$  the angular distribution exhibits a sequence of broad but well defined maxima, while for systems with high valence the angular distribution is much less structured.

For patchy colloids with highly directional bonds, the orientation of the colloids on the substrate is of major importance. The orientation of the colloids in the network depends on the orientational distribution of the first layer. Orientation of the patches close to the vertical favors the growth of the network by minimizing the blocking effects of colloids in the next layer. Sustained growth is favored by the vertical alignment of one patch, since vertically growing aggregates are favored over diagonally and laterally growing ones, or maximal exposure of the patches, since aggregates with more exposed patches are more likely to grow. Geometrical constraints lead to a strong dependence on  $n$ . For  $n = 3$ , Fig.9(a), the preferred orientation of the bonds is  $\gamma = 2\pi/3$  or  $\gamma = \pi$ , corresponding to colloids with one patch aligned with the  $y$  axis or two patches at an angle on either sides of the  $y$  axis. For  $n = 4$ , the distribution function has a maximum at  $\gamma = 3\pi/4$ , Fig. 9(a), which corresponds to colloids with two patches at an angle on either sides of the  $y$  axis. In this case the second condition dominates. For colloids with  $n = 5$  the distribution function, Fig. 9(a), has three maxima indicating that three patches are exposed to newly incoming colloids. The first maximum is just above  $\gamma = \pi/2$  and thus one patch is aligned with the  $x$  axis. For systems with  $n = 6$  the alignment is similar to that of three-patch colloids. Up to four patches may be exposed but symmetry reduces the number of maxima of the distribution function to two.

Maximal exposure of the free patches determines the preferred orientation(s) of colloids in networks of low valence colloids. These are indicated by maxima in Fig. 9(a) which become less visible for  $n > 6$ , Fig. 9(b).

## IV. CONCLUSIONS

We studied the aggregation of patchy colloids on substrates and characterized the dependence of the bulk and interfacial properties on the number of patches. We have shown that regardless of the number of patches the interface is always in the *Kardar-Parisi-Zhang* class in contrast to what is observed for selective interaction between patches [38]. We found that the roughness depends on the number of patches with a minimum at  $n = 4$ , which is similar to what occurs by introducing patch-patch correlations on three-patch colloids [37].

In addition, we studied the influence of the number of patches on the bulk structure of the film. We have shown that low-valence colloids aggregate into ordered structures ( $n \leq 6$ ) which extend over distances much

larger than the diameter of the particles. We found that the local structure of the aggregates and the bulk density depend on the number of patches in a non-monotonic fashion. This effect is different to what was reported for mixtures of colloids. In that case, the density increases monotonically with the valence, both under equilibrium [14, 48] and nonequilibrium [36] conditions.

Finally, we measured the orientation of the bonds between patches and found that the valence provides control over the directionality of bonds and on the relative growth of the aggregates. This has relevance to the growth of mixtures of patchy colloids of type *A* and *B*

with *n* patches each, where *n* may be used to tune, for example, the directionality of dipoles created by the bonds between *A*- and *B*-type colloids. Also the control over the direction of conducting circuits created by bonds of patchy colloids could have practical interest.

## ACKNOWLEDGMENTS

We acknowledge financial support from the Portuguese Foundation for Science and Technology (FCT) under Contracts nos. EXCL/FIS-NAN/0083/2012, PEst-OE/FIS/UI0618/2014, and IF/00255/2013.

- 
- [1] A.B. Pawar and I. Kretzschmar, *Macromol. Rapid Commun.* **31**, 150 (2010).
- [2] I. Kretzschmar and J.H. Song, *Curr. Opin. Coll. Interf. Sci.* **16**, 84 (2011).
- [3] S. Sacanna and D.J. Pine, *Curr. Opin. Coll. Interf. Sci.* **16**, 96 (2011).
- [4] E. Bianchi, R. Blaak and C.N. Likos, *Phys. Chem. Chem. Phys.* **13**, 6397 (2011).
- [5] G.R. Yi, D.J. Pine and S. Sacanna, *J. Phys.: Condens. Matter* **25**, 193101 (2013).
- [6] O.I. Wilner and I. Willner, *Chem. Rev.* **112**, 2528 (2012).
- [7] J. Hu, S. Zhou, Y. Sun, X. Fang and L. Wu, *Chem. Soc. Rev.* **41**, 4356 (2012).
- [8] E. Duguet, A. Désert, A. Perro and S. Ravaine, *Chem. Soc. Rev.* **40**, 941 (2011).
- [9] H.C. Shum, A.R. Abate, D. Lee, A.R. Studart, B. Wang, C.H. Chen, J. Thiele, R.K. Shah, A. Krummel and D.A. Weitz, *Macromol. Rapid Commun.* **31**, 108 (2010).
- [10] Y. Wang, D.R. Breed, V.N. Manoharan, L. Feng, A.D. Hollingsworth, M. Weck and D.J. Pine, *Nature* **491**, 51 (2012).
- [11] Z. He and I. Kretzschmar, *Langmuir* **28**, 9915 (2012).
- [12] Z. Zhang and S.C. Glotzer, *Nano Lett.* **4**, 1407 (2004).
- [13] B. Ruzicka, E. Zaccarelli, L. Zulian, R. Angelini, M. Sztucki, A. Moussaïd, T. Narayanan and F. Sciortino, *Nature Mater.* **10**, 56 (2010).
- [14] E. Bianchi, J. Largo, P. Tartaglia, E. Zaccarelli and F. Sciortino, *Phys. Rev. Lett.* **97**, 168301 (2006).
- [15] J. Russo and F. Sciortino, *Phys. Rev. Lett.* **104**, 195701 (2010).
- [16] J. Russo, P. Tartaglia and F. Sciortino, *J. Chem. Phys.* **131**, 014504 (2009).
- [17] F. Sciortino and E. Zaccarelli, *Curr. Opin. Solid State Mater. Sci.* **15**, 246 (2011).
- [18] F. Sciortino, E. Bianchi, J.F. Douglas and P. Tartaglia, *J. Chem. Phys.* **126**, 194903 (2007).
- [19] S. Sokolowski and Y.V. Kalyuzhnyi, *J. Phys. Chem. B* **118**, 9076 (2014).
- [20] O. Pizio, S. Sokolowski and Z. Sokolowska, *J. Chem. Phys.* **140**, 174706 (2014).
- [21] G. Doppelbauer, E. Bianchi and G. Kahl, *J. Phys.: Cond. Matter* **22**, 104105 (2010).
- [22] B.D. Marshall and W.G. Chapman, *J. Chem. Phys.* **139**, 054902 (2013).
- [23] B.D. Marshall and W.G. Chapman, *Phys. Rev. E* **87**, 052307 (2013).
- [24] J.M. Tavares, N.G. Almarza and M.M. Telo da Gama, *J. Chem. Phys.* **140**, 044905 (2014).
- [25] O. Markova, J. Alberts, E. Munro and P.F. Lenne, *Phys. Rev. E* **90**, 022301 (2014).
- [26] Y. Iwashita and Y. Kimura, *Soft Matt.* **9**, 10694 (2013).
- [27] Y. Iwashita and Y. Kimura, *Soft Matt.* **10**, 7170 (2014).
- [28] F. Sciortino, C. De Michele, S. Corezzi, J. Russo, E. Zaccarelli and P. Tartaglia, *Soft Matter* **5**, 2571 (2009).
- [29] S. Corezzi, C. De Michele, E. Zaccarelli, P. Tartaglia and F. Sciortino, *J. Phys. Chem. B* **113**, 1233 (2009).
- [30] S. Corezzi, D. Fioretto and F. Sciortino, *Soft Matt.* **8**, 11207 (2012).
- [31] O.A. Vasilyev, B.A. Klumov and A.V. Tkachenko, *Phys. Rev. E* **88**, 012302 (2013).
- [32] N. Gnan, D. de Las Heras, J.M. Tavares, M.M. Telo da Gama and F. Sciortino, *J. Chem. Phys.* **137**, 084704 (2012).
- [33] N.R. Bernardino and M.M. Telo da Gama, *Phys. Rev. Lett.* **109**, 116103 (2012).
- [34] C.S. Dias, N.A.M. Araújo and M.M. Telo da Gama, *Phys. Rev. E* **87**, 032308 (2013).
- [35] C.S. Dias, N.A.M. Araújo and M.M. Telo da Gama, *Soft Matter* **9**, 5616 (2013).
- [36] C.S. Dias, N.A.M. Araújo and M.M. Telo da Gama, *J. Chem. Phys.* **139**, 154903 (2013).
- [37] C.S. Dias, N.A.M. Araújo and M.M. Telo da Gama, *Phys. Rev. E* **90**, 032302 (2014).
- [38] C.S. Dias, N.A.M. Araújo and M.M. Telo da Gama, *EPL* **107**, 56002 (2014).
- [39] P. Meakin, *Fractals, scaling and growth far from equilibrium* (Cambridge Univ Pr, Cambridge, 1998).
- [40] M.J. Vold, *J. Colloid Sci.* **695**, 684 (1963).
- [41] M.J. Vold, *J. Colloid Sci.* **14**, 168 (1959).
- [42] N. Geerts and E. Eiser, *Soft Matt.* **6**, 4647 (2010).
- [43] M.E. Leunissen and D. Frenkel, *J. Chem. Phys.* **134**, 084702 (2011).
- [44] P.J. Yunker, M.A. Lohr, T. Still, A. Borodin, D.J. Durian and A.G. Yodh, *Phys. Rev. Lett.* **110**, 035501 (2013).
- [45] A.L. Barabási and H.E. Stanley, *Fractal Concepts in Surface Growth* (Cambridge University Press, Cambridge, 1995).
- [46] G. Ódor, *Rev. Mod. Phys.* **76**, 663 (2004).
- [47] F. Family and T. Vicsek, *J. Phys. A: Math. Gen.* **18**, L75 (1985).

- [48] D. de las Heras, J.M. Tavares and M.M. Telo da Gama, *Soft Matt.* **7**, 5615 (2011).